J. Fluid Mech. (1977), *vol.* 81, *part* 3, *pp.* 593–607
Printed in Great Britain

An inviscid bluff-body wake model which includes the far-wake displacement effect

By MASARU KIYA AND MIKIO ARIE
Faculty of Engineering, Hokkaido University,
Sapporo, 060 Japan

(Received 12 July 1976)

This paper presents an inviscid bluff-body wake model which correctly takes into account the displacement effect of the far wake by means of an appropriate source–sink system located behind the body. The separating streamlines, which in previous inviscid wake models have been regarded as the time-averaged shear layers emanating from the separation points within a small distance downstream of the body, can be interpreted as the displacement surface of the wake throughout the whole region of flow behind the body. The solutions for a normal flat plate, a circular cylinder and a 90° wedge are worked out and compared with experiments, where possible. The theoretical pressure distributions agree fairly well with the experimental ones. The shape of the separating streamlines obtained from the present theory is physically reasonable and compares well with experimental results for a normal plate and a 90° wedge.

1. Introduction

The time-averaged characteristics of the separated flow over a two-dimensional bluff body at sufficiently large Reynolds numbers have been treated theoretically by means of free-streamline theories in which an inviscid fluid is assumed. The free-streamline theories were initiated by Helmholtz and Kirchhoff, who considered two-dimensional incompressible flow past flat plates under the assumption that the pressure everywhere in the wake was equal to the pressure outside the wake at infinity. Some modifications of the Helmholtz–Kirchhoff model to allow arbitrary base pressures were made by Roshko (1954), Wu (1962), Woods (1955) and Parkinson & Jandali (1970) among others. A good review of the free-streamline theories and related characteristics of the wake flows was written by Wu (1972). If the base-pressure coefficient and the location of the separation points are assigned on the basis of experimental information, these theories give pressure distributions around bluff bodies in good agreement with experimental measurements.

In these theories the dividing streamlines emanating from the separation points have been assumed to represent the approximate shapes of the separated shear layers or the time-averaged boundary of the wake bubbles. Actually, within a short distance downstream of the separation points, the dividing streamlines calculated by these theories agree fairly well with the time-averaged shear layers obtained experimentally for some typical bluff bodies such as a flat plate or a circular cylinder. From the physical point of view, the dividing streamlines far downstream of the body should represent

the displacement surface of the wake, which is related to the drag force exerted on the body through the momentum principle. This concept was originally put forward by Woods (1961).† However, he did not actually use this criterion to determine the velocity distribution on the free streamlines of his models. The reason for this is that the rough approximation of the far wake will not have a dominant influence on the flow field near the body, although the latter is one of the main objectives of the free-streamline theories.

However, in order to make the free-streamline theories physically more realistic, it is desirable that the dividing streamlines far downstream of the body should coincide with the displacement surface of the far wake. A flow model of this type will yield a first-order approximation to the irrotational flow field outside the wake over the whole region from the near wake to the far wake. From the practical point of view, the irrotational flow field due to the displacement effect of the wake may be useful for assessing the wake blockage effect, which sometimes becomes important in a wind-tunnel experiment (Pankhurst & Holder 1952). It is the purpose of this paper to present a free-streamline theory which correctly takes into account the displacement effect of the far wake by means of a source–sink system located behind the body. The theoretical predictions are compared with experiments where possible.

2. Mathematical formulation of the model

The wake source model of Parkinson & Jandali (1970) will be used with a few modifications required to incorporate the wake displacement effect into the framework of the present theory. The present theory is thus an extension of their theory.

Consider two-dimensional, incompressible, irrotational, steady flow, uniform at infinity, past a body symmetrical with respect to the incident flow, and with symmetrical separation at S_1 and S_2 in the z plane ($z = x+iy$), as shown in figure 1. The upstream part S_1AS_2 of the body contour AS_1CS_2A is mapped conformally from the corresponding part of a circle of radius a in the Z plane ($Z = X+iY$) by the analytic function

$$z = f(Z), \tag{1}$$

where the points S_1 and S_2 are critical points at which the derivative $f'(Z)$ has simple zeros. The angle of intersection of curves is doubled at S_1 and S_2 in the z plane and the complete circle in the Z plane is mapped onto the slit AS_1BS_2A in the z plane. The part of the actual body contour downstream of the separation points, which is represented by S_1CS_2 in the z plane, is ignored in the present analysis. The separation points in the Z plane are located at

$$Z_{S_1} = a\,e^{i\alpha}, \quad Z_{S_2} = a\,e^{-i\alpha}, \tag{2}$$

where α is a real constant. Assume that the function $f(Z)$ satisfies

$$f(Z) = k_1^{-1}Z + O(Z^0) \quad \text{as} \quad |Z| \to \infty, \tag{3}$$

where k_1 is a constant. For a symmetrical transformation such as that shown in figure 1, k_1 will become a real constant.

† The authors are grateful to a referee for pointing out that Woods considered this problem in his book published in 1961.

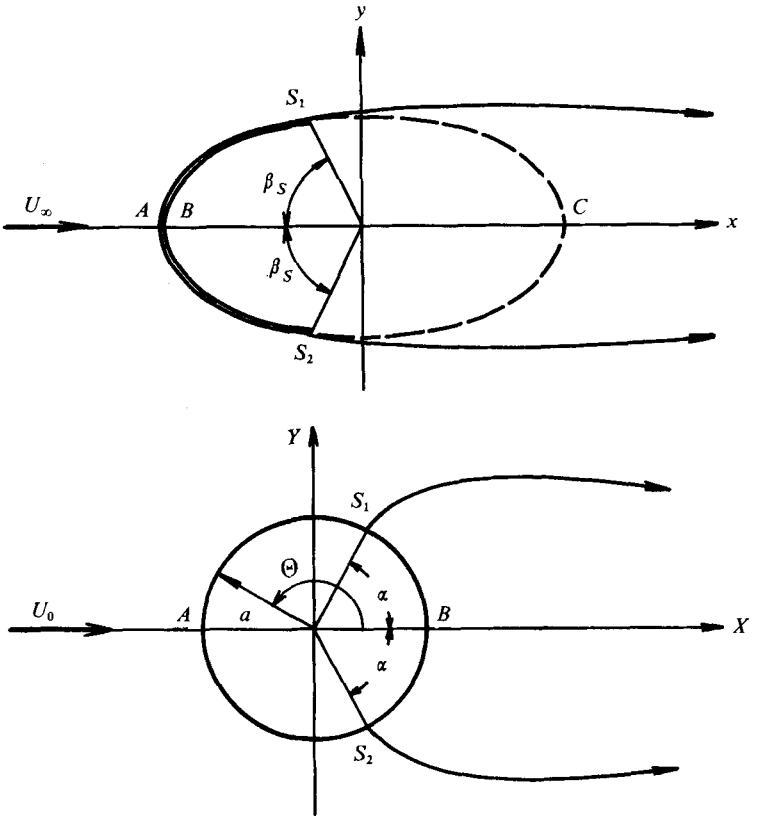

FIGURE 1. Physical and transform planes.

The basic flow past the circle in the Z plane is the familiar combination of uniform flow in the direction of the X axis and flow from a suitable doublet at the origin. The complex potential W_u of the basic flow is given by

$$W_u = U_0(Z + a^2/Z), \tag{4}$$

where U_0 is the velocity of the incident flow in the Z plane. Accordingly, the incident-flow velocity in the z plane is $k_1 U_0$, which will hereafter be referred to as U_∞.

In order to have free streamlines emanating from the separation points S_1 and S_2, one adds to this basic flow two sources of strengths Q_1 and Q_2 located on the real axis of the Z plane at $(a, 0)$ and $(a e^{\beta}, 0)$, β being a positive constant, together with their image sources and sinks located in the interior of the circle. This arrangement of sources is selected solely on the basis of simplicity. It may be remarked that an arrangement of two sources along the rear side of the circle, i.e. the arc $S_1 B S_2$ on the Z plane in figure 1, is another source arrangement which deserves attention from the point of view of simplicity. However, a few calculations revealed that the source arrangement along the X axis could be applied to a larger number of bluff bodies than that along the rear side of the circle. The complex potential of the source–sink system which satisfies the boundary condition on the surface of the circle is

$$W_Q = (2\pi)^{-1} Q_1 \log\{(Z-a)^2/Z\} + (2\pi)^{-1} Q_2 \log\{(Z^2 - 2aZ\cosh\beta + a^2)/Z\}. \tag{5}$$

The resulting flow can be described by the complex potential

$$W = W_u + W_Q. \tag{6}$$

The complex velocity w in the z plane is given by

$$w^* = u - iv = (dW/dZ)/f'(Z), \tag{7}$$

where the asterisk means the complex conjugate and u and v are the velocity components in the x and y directions respectively. As mentioned previously, the points S_1 and S_2 are the critical points of the transformation given by (1), where $f'(Z)$ has simple zeros. Therefore, in order that the velocities at the points S_1 and S_2 will be finite, one must have

$$dW/dZ = 0 \quad \text{at} \quad Z = Z_{S_1} \quad \text{and} \quad Z_{S_2}. \tag{8}$$

Because of the doubling of the angles at the critical points, the stagnation streamlines leaving S_1 and S_2 in the Z plane become the tangential separation streamlines at S_1 and S_2 in the z plane. Since the flow is symmetrical with respect to the real axes of the complex planes, the conditions at either of the points S_1 and S_2 will suffice to determine the parameters of the flow. In the following analysis the conditions at the point S_1 will be considered. From (4)–(6) one obtains

$$\begin{aligned} dW/dZ = U_0\{1 - (a^2/Z^2)\} + (2\pi)^{-1}Q_1(Z+a)/\{Z(Z-a)\} \\ + (2\pi)^{-1}Q_2(Z^2 - a^2)/\{Z(Z^2 - 2aZ\cosh\beta + a^2)\}. \end{aligned} \tag{9}$$

Accordingly, substitution of (9) into (8) yields

$$Q_1/(\cos\alpha - 1) + Q_2/(\cos\alpha - \cosh\beta) = -4\pi a U_0, \tag{10}$$

which is one of the conditions to be satisfied by the three parameters Q_1, Q_2 and β.

The velocity at the separation point can be calculated from

$$w^*_{S_1} = [(d^2W/dZ^2)/f''(Z)]_{S_1}, \tag{11}$$

where the right-hand side is evaluated at the point S_1 in the Z plane. Substituting (9) into (11) and taking into account the relation (10), one obtains

$$w^*_{S_1} = I e^{-2i\alpha}\sin^2\alpha/\{2\pi a^2 f''(Z_{S_1})\}, \tag{12a}$$

where

$$I = Q_1/(\cos\alpha - 1)^2 + Q_2/(\cos\alpha - \cosh\beta)^2. \tag{12b}$$

The magnitude of the velocity at the separation point is thus given by

$$q_{S_1} = I\sin^2\alpha/\{2\pi a^2 n|f''(Z_{S_1})|\}, \tag{13}$$

in which $n = \pm 1$ if $I \gtrless 0$. In the same manner as in the free-streamline theories mentioned above, the flow is assumed to separate at the empirical value of the base-pressure coefficient, which is defined by

$$C_{pb} = (p_b - p_\infty)/(\tfrac{1}{2}\rho U_\infty^2), \tag{14}$$

where p_b is the base pressure and p_∞ is the pressure infinitely far upstream. The flow inside the separation streamline is ignored and the pressure coefficient over the downstream face S_1CS_2 in the z plane is assumed constant and equal to C_{pb}. Writing $q_{S_1} = kU_\infty$, where

$$k = (1 - C_{pb})^{\frac{1}{2}}, \tag{15}$$

one obtains from (13)

$$Q_1/(\cos\alpha-1)^2+Q_2/(\cos\alpha-\cosh\beta)^2 = 2\pi a^2 n|f''(Z_{S_1})|kU_\infty/\sin^2\alpha. \tag{16}$$

This is the second condition imposed on the three parameters.

One now incorporates the displacement effect of the far wake in the present flow model. It is well known that the presence of the far wake is associated with a source-like contribution to the irrotational flow field outside the wake, the strength of the effective source being

$$D/(\rho U_\infty), \tag{17}$$

where D is the drag force exerted on the body (Batchelor 1967, §5.12). The flow at large distances from the body is evidently a superposition of a uniform stream and the flow due to a source whose strength is given by (17). Accordingly, the total strength of the sources outside the circle in the Z plane must satisfy the condition

$$\rho U_\infty(Q_1+Q_2) = D. \tag{18}$$

If the drag coefficient C_D is defined by

$$C_D = D/(\tfrac{1}{2}\rho U_\infty^2 l), \tag{19}$$

as usual, where l is a representative length of the body, (18) can also be written as

$$Q_1+Q_2 = \tfrac{1}{2}C_D U_\infty l. \tag{20}$$

This is the third condition imposed on the source arrangement. It should be mentioned that Woods (1961, §11.1) gave a criterion equivalent to (20) but did not in fact use that criterion in determining the velocity distribution along the free streamlines of his wake models. To the authors' knowledge, this is the first time that the relation (20) has been introduced into the actual framework of an inviscid wake model. Equations (10), (16) and (20) are the simultaneous equations from which the three parameters Q_1, Q_2 and β are to be determined.

Since (10) and (16) allow Q_1 and Q_2 to be obtained in terms of β, substitution of the resulting expressions for Q_1 and Q_2 into (20) yields a transcendental equation for β, which includes the drag coefficient C_D as an unknown parameter. Accordingly, a value of C_D must be assumed to begin with. Then the resulting values of β, Q_1 and Q_2 will yield the pressure distribution along the wetted surface of the body, which can be integrated to obtain the drag coefficient. Unless the calculated drag coefficient is equal to the assumed value to the required accuracy, the same process must be repeated until convergence is attained. For a few typical bluff bodies which will be described later, in §4, sufficient convergence was obtained after two or three iterations.

Partly from a few results of calculations and partly from physical reasoning, it is conjectured that Q_1 and Q_2 must be positive and negative respectively in order for the present theory to yield a reasonable flow pattern around the body. In view of (10) and (16), this condition reduces to

$$|f''(Z_{S_1})| > 2(1+\cos\alpha)/(nakk_1), \tag{21}$$

which is found to hold with a sufficient margin for some typical two-dimensional bluff bodies such as a normal flat plate, a circular cylinder and an elliptical cylinder.

The complex velocity w_f on the wetted surface of the body can be obtained by substituting (9) into (7) and putting $Z = a\exp(i\Theta)$ $(\alpha < \Theta \leqslant \pi)$ in the resulting equation, the final form being

$$w_f^* = \{i e^{-i\Theta}\sin\Theta/f'(a e^{i\Theta})\}(2U_0+(2\pi a)^{-1}\{Q_1/(\cos\Theta-1)+Q_2/(\cos\Theta-\cosh\beta)\}). \tag{22}$$

The pressure coefficient on the wetted surface of the body is thus given by

$$C_p = 1 - w_f w_f^*/U_\infty^2. \tag{23}$$

3. Conditions at separation points

In the theory developed in § 2, the separation points, which are represented by an angle α in the Z plane, and the base-pressure coefficient C_{pb} are specified empirically, and while the theory gives separating streamlines which are tangential to the body surface at separation, it does not specify their curvature there. Knowledge of the curvature is important because of the possibility of physically inadmissible solutions in which the predicted separating streamlines intersect the body surface downstream of separation.

As demonstrated by Woods (1961, § 11.6, information on the streamline curvature just after separation can be obtained by examining $\partial C_p/\partial s$ (where s is the distance measured from the forward stagnation point along the body surface) on the wetted surface of the body near the separation points. Since C_p and s are both functions of Θ, one obtains

$$(\partial C_p/\partial s)_{S_1} = (\partial C_p/\partial \Theta)_{S_1}/(\partial s/\partial \Theta)_{S_1}. \tag{24}$$

From the correspondence between the z and Z planes illustrated in figure 1, it is clear that

$$\partial s/\partial \Theta < 0 \quad \text{on} \quad AS_1, \quad \partial s/\partial \Theta = 0 \quad \text{at} \quad S_1. \tag{25a,b}$$

In order to obtain $(\partial C_p/\partial s)_{S_1}$, one examines the behaviour of $\partial C_p/\partial s$ near S_1. If Θ is written as $\Theta = \alpha + \epsilon$ $(0 < \epsilon \ll \alpha)$, w_f^* can be expanded in the form

$$w_f^* = \frac{1}{c_1}\left(2P_1 d_1 + \epsilon\left\{2P_1\left(d_2 + d_1\frac{c_2}{2c_1}\right) - P_1 d_2\right\}\right) + O(\epsilon^2), \tag{26}$$

where

$$P_1 = U_0\cos\alpha - (4\pi a)^{-1}Q_1/(\cos\alpha - 1) + (4\pi a)^{-1}Q_2(1 - \cos\alpha\cosh\beta)/(\cos\alpha - \cosh\beta)^2, \tag{27a}$$

$$P_2 = U_0\sin\alpha + (4\pi a)^{-1}\sin\alpha\{Q_1/(\cos\alpha - 1)^2 - Q_2(2 - \cosh^2\beta - \cos\alpha\cosh\beta)/(\cos\alpha - \cosh\beta)^3\}, \tag{27b}$$

$$c_1 = i e^{i\alpha} a f''(Z_{S_1}), \quad c_2 = a e^{i\alpha} f''(Z_{S_1}) + a^2 e^{2i\alpha} f'''(Z_{S_1}), \tag{27c}$$

$$d_1 = i e^{-i\alpha}, \quad d_2 = e^{-i\alpha}. \tag{27d}$$

In view of the relations $d_1 d_2^* + d_1^* d_2 = 0$ and $d_1 d_1^* = 1$, the square $w_f w_f^*$ of the magnitude of the velocity becomes

$$w_f w_f^* = \frac{2P_1}{c_1 c_1^*}\left(2P_1 + \epsilon\left\{P_1\left(\frac{c_2}{c_1} + \frac{c_2^*}{c_1^*}\right) - 2P_2\right\}\right) + O(\epsilon^2).$$

Accordingly, one obtains from (23)

$$\left(\frac{\partial C_p}{\partial \Theta}\right)_{S_1} = -\left(\frac{\partial}{\partial \epsilon}\frac{w_f w_f^*}{U_\infty^2}\right)_{\epsilon=0} = -\frac{4P_1}{U_\infty^2 c_1 c_1^*}(mP_1 - P_2), \tag{28}$$

where

$$m = \tfrac{1}{2}\{(c_2/c_1) + (c_2^*/c_1^*)\}. \tag{29}$$

From (24), (25) and (28), it follows that

$$(\partial C_p/\partial s)_{S_1} = \begin{cases} +\infty & \text{for} \quad P_1(mP_1 - P_2) > 0, \\ \text{finite} & \text{for} \quad P_1(mP_1 - P_2) = 0, \\ -\infty & \text{for} \quad P_1(mP_1 - P_2) < 0. \end{cases}$$

If $(\partial C_p/\partial s)_{S_1} = -\infty$, it can be shown (Woods 1961, §11.1) that the curvature of the separation streamline at S_1 is infinite and convex when viewed from outside the wake, so that the streamline would intersect the cylinder. Therefore any solution with $P_1(mP_1 - P_2) < 0$ is physically inadmissible. On the other hand, if $P_1(mP_1 - P_2) > 0$ there is an infinite adverse pressure gradient at S_1, which is not possible because separation would have already taken place in view of the characteristics of the boundary layer along the body surface. Thus, in order to obtain a finite pressure gradient and streamline curvature at the separation points, the following equation must be satisfied:

$$P_1(mP_1 - P_2) = 0.$$

This is the 'smooth-separation' condition and it enables a relation between the base pressure and the position of the separation point to be determined. Since P_1 cannot be zero in view of the relation

$$P_1 = \tfrac{1}{2} q_{S_1} na |f''(Z_{S_1})|, \tag{30}$$

the above equation yields

$$mP_1 - P_2 = 0. \tag{31}$$

Substituting (27*a*, *b*) into (31), one obtains

$$Q_1\left(\frac{m\sin\alpha}{(\cos\alpha-1)^2}+\frac{\cos\alpha-2}{(\cos\alpha-1)^2}\right)+Q_2\left(\frac{m\sin\alpha}{(\cos\alpha-\cosh\beta)^2}+\frac{2-3\cos\alpha\cosh\beta+\cos^2\alpha}{(\cos\alpha-\cosh\beta)^3}\right)=0. \tag{32}$$

In this case the constants Q_1, Q_2 and β must be determined through the use of (10), (20) and (32), while (16) yields the value of k.

As will be shown in § 4.2, the angle of separation thus obtained for a circular cylinder is much less than the value obtained if k is determined empirically, so that the theoretical pressure distribution is inaccurate near the actual separation point. This result is not a matter of surprise in view of the fact that the smooth-separation condition does not take into account the actual near-wake dynamics, which are of vital importance in the determination of the base pressure and the separation point. Accordingly, from the practical point of view, the requirement of finite curvature should be abandoned; both the base pressure and the separation point are chosen empirically as discussed in § 2. From a few calculations it is found that $(\partial C_p/\partial s)_{S_1}$ becomes positively infinite for a number of smooth cylinders without salient edges so long as the separation point occurs sufficiently far downstream of the forward stagnation point.

Some examples are now worked out and compared with other theoretical and experimental results.

4. Applications

4.1. *Normal flat plate*

The mapping function $f(Z)$ is given by

$$f(Z) = Z - a^2/Z, \tag{33}$$

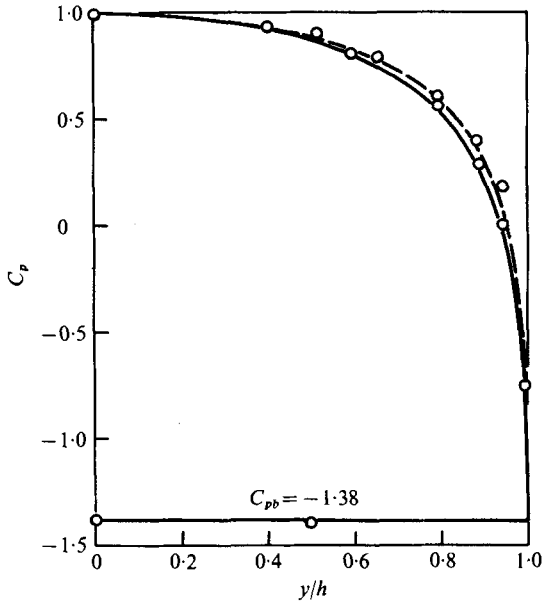

FIGURE 2. Pressure distribution on a normal flat plate. ——, present theory, $C_D = 2{\cdot}11$; – – –, theory of Parkinson & Jandali (1970), $C_D = 2{\cdot}13$; ○, experiment of Fage & Johansen (1927), $C_D = 2{\cdot}13$. y is distance measured from forward stagnation point and $2h$ is height of plate.

which yields a normal flat plate of height $2h = 4a$ in the physical plane. Since $k_1 = 1$, $\alpha = \frac{1}{2}\pi$, $Z_{S_1} = ai$ and $f''(Z_{S_1}) = -2i/a$ in this case, (10), (16) and (20) become

$$Q_1 + Q_2/\cosh\beta = 4\pi a U_0, \quad Q_1 + Q_2/\cosh^2\beta = 4\pi a k U_0,$$

$$Q_1 + Q_2 = 2C_D U_0 a,$$

in which $n = 1$ has been employed. From (22), the velocity on the front surface of the plate becomes

$$w_f^* = i\tan\Theta\left[U_0 + \frac{1}{4\pi a}\left(\frac{Q_1}{\cos\Theta - 1} + \frac{Q_2}{\cos\Theta - \cosh\beta}\right)\right]. \tag{34}$$

Figure 2 shows the pressure distribution on the front surface of the plate obtained from the present theory together with the experimental result of Fage & Johansen (1927) and another theoretical curve given by Parkinson & Jandali (1970). Although the present theory predicts a slightly lower pressure on the front surface of the plate, the difference between the two theoretical curves is very small and their agreement with the experiment is good. In figure 3 the theoretical flow pattern around the plate is compared with the experimental result of Arie & Rouse (1956). Since the separation streamline obtained from the present theory should be interpreted as the displacement surface of the wake, the experimental displacement surface which is obtained from the flow pattern given by Arie & Rouse is also included in figure 3. From this result the present theory may be found to provide a fairly good first-order approximation to the displacement surface of the wake. Recently Bradbury (1976) measured the wake bubble behind a normal flat plate by means of a pulsed hot wire. His wake-bubble shape is almost identical to that of Arie & Rouse except that the stagnation point of his wake bubble appears at about $x/h = 4$ whereas theirs is located at $x/h = 4{\cdot}4$.

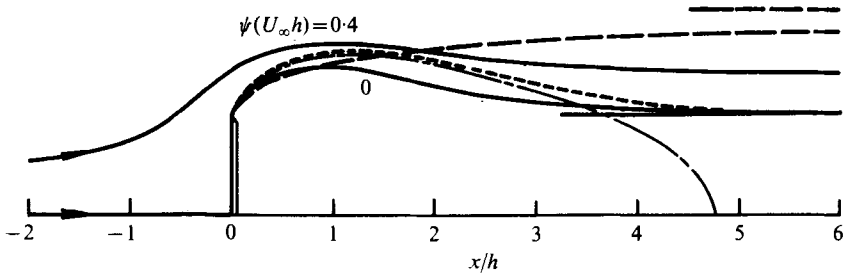

FIGURE 3. Flow patterns around a normal flat plate. ——, present theory; – – –, theory of Parkinson & Jandali (1970); ····, experimental displacement surface (Arie & Rouse 1956); —·—, experimental wake-bubble boundary (Arie & Rouse 1956). Horizontal lines parallel to x axis show asymptotic downstream height of separation streamlines.

Accordingly the displacement surface obtained from Bradbury's measurement will approach its asymptote more rapidly than will the displacement surface of Arie & Rouse, thus yielding better agreement between the theory and experiment. In passing it should be mentioned that the smooth-separation condition cannot be applied in this case because of the infinite curvature at the edges of the plate.

4.2. *Circular cylinder*

If the radius of the circular cylinder represented by a circular arc $S_1 A S_2$ in the z plane is chosen as unity, the mapping function is given by

$$f(Z) = Z - a^2 - a^2(1-a^2)/(Z-a^2), \tag{35}$$

in which a is a constant related to the separation angle β_S and α by

$$\alpha = \tfrac{1}{2}(\pi - \beta_S), \quad a = \cos\alpha. \tag{36a,b}$$

From (35) one easily obtains

$$k_1 = 1, \quad f''(Z_{S_1}) = -2i/(a\sin\alpha),$$

$$f'''(Z_{S_1}) = 6/\{a^2(1-a^2)\}, \quad m = 3\cot\alpha.$$

Through the use of these quantities, the three parameters Q_1, Q_2 and β can be calculated from (10), (16) and (20) or from (10), (20) and (32) in the case of the smooth-separation condition.

Figures 4–7 show comparisons of results of the present theory with theoretical results of Parkinson & Jandali (1970) and with experimental results of Roshko (1954, 1961) and Bearman (1968). Figures 4 and 5 show the surface pressure distributions in the subcritical, critical and transcritical Reynolds number ranges respectively. For the same separation angles and base-pressure coefficients, the present theory yields higher suction peaks than that of Parkinson & Jandali. Thus the overall agreement between the present theory and the experiments is less satisfactory. However, if somewhat smaller separation angles are chosen, the present theory gives similarly good agreement with the experimental measurements.

Figure 4 also shows the theoretical pressure distributions obtained by applying the smooth-separation condition (32). For the experimental base-pressure coefficient $C_{pb} = -0{\cdot}96$ ($k = 1{\cdot}40$), the present theory predicts the separation point to be at

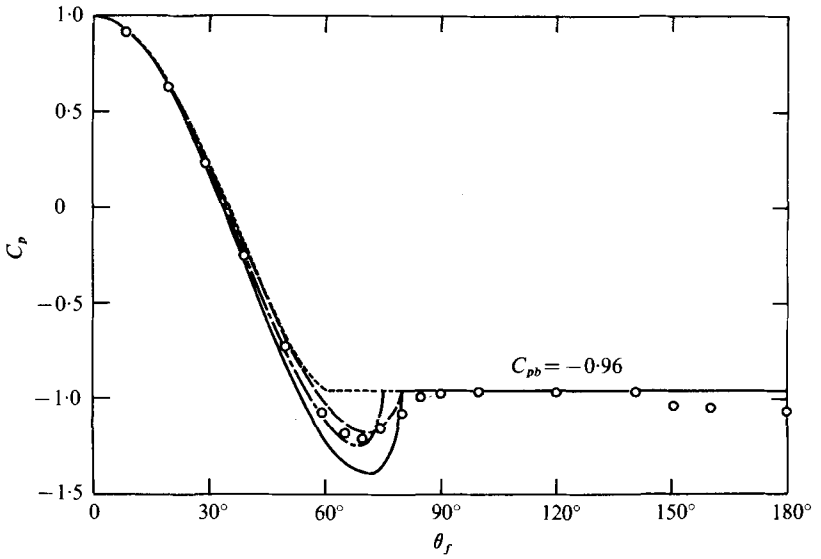

FIGURE 4. Pressure distribution on a circular cylinder (subcritical flow regime). ——, present theory, $\beta_S = 80°$, $C_D = 0{\cdot}97$; —·—, present theory, $\beta_S = 75{\cdot}0°$, $C_D = 1{\cdot}01$; ·····, present theory, smooth-separation condition, $\beta_S = 60{\cdot}8°$, $C_D = 1{\cdot}06$; – – –, theory of Parkinson & Jandali (1970), $\beta_S = 80°$, $C_D = 1{\cdot}09$; ○, experiment of Roshko (1954), Reynolds number $= 1{\cdot}54 \times 10^4$, $C_D = 1{\cdot}07$. θ_f is angle measured from forward stagnation point.

$\beta_S = 60{\cdot}8°$, while for the experimental laminar separation angle $\beta_S = 80°$, it yields a base-pressure coefficient of $C_{pb} = -1{\cdot}72$. Accordingly, as may be seen in figure 4, the corresponding theoretical pressure distributions are inaccurate near the actual separation point. For the critical and transcritical flow regimes, values of the parameters Q_1, Q_2 and β which satisfy the smooth-separation condition could not be obtained.

Figures 6 and 7 give the separation-streamline shapes calculated from the present theory together with the theoretical results of Parkinson & Jandali (1970). Although the two theoretical separation streamlines lie close together in the neighbourhood of the separation point, the asymptotic downstream spacing given by the present theory is appreciably smaller than that given by the theory of Parkinson & Jandali. This is the main consequence of condition (20). Figure 6 also includes an experimental flow pattern around a circular cylinder which was constructed from a flow-visualization photograph taken by Igarashi (1975) in an air tunnel with smoke, the Reynolds number being $1{\cdot}38 \times 10^4$. Since the exposure time is 1·0 s and the velocity of the approaching stream is 6·0 m/s, the flow pattern corresponds to a time-averaged flow pattern around the cylinder. In fact the vortex-shedding frequency is about 35 Hz in this experiment. Although the exact displacement surface of the wake is not clear in this experimental flow pattern, it may be conjectured that the predicted approach of the displacement surface to its asymptote is more rapid than the experimental one. Detailed measurement of the mean velocity distribution in the near wake is required to obtain the exact shape of the displacement surface, and thus the assessment of the present theory in this respect may still be incomplete owing to the lack of any such experimental information which is reliable.

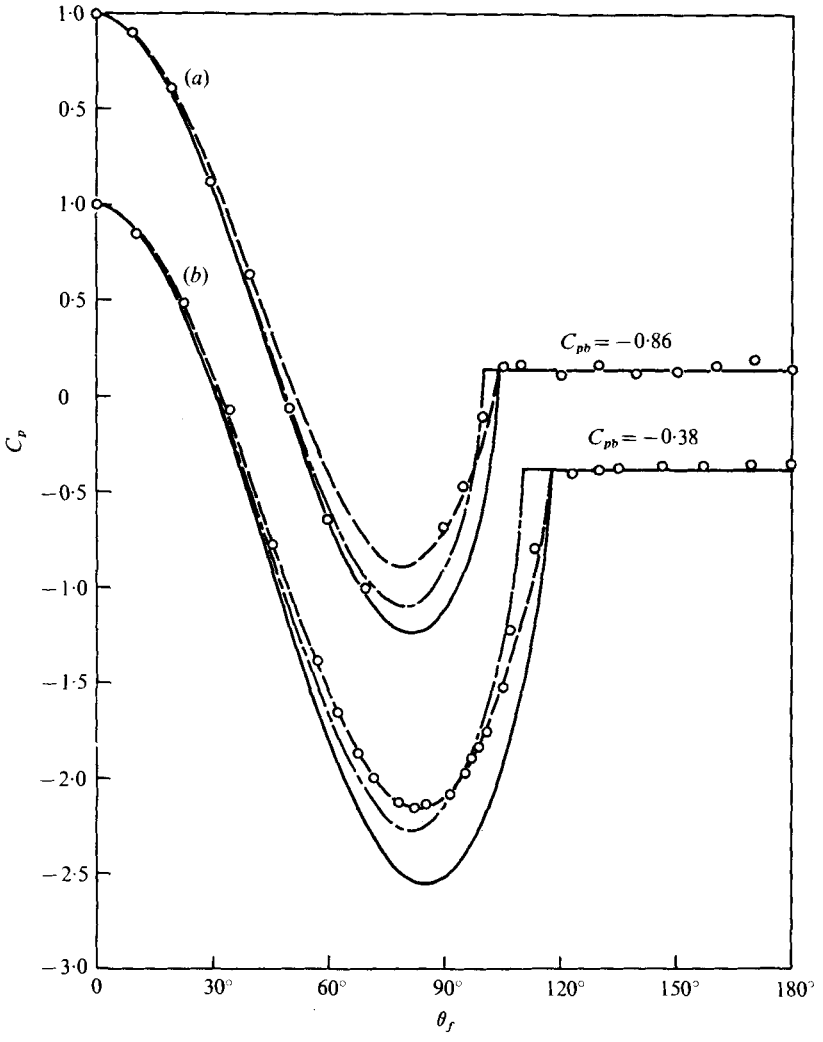

FIGURE 5. Pressure distribution on a circular cylinder. (*a*) Transcritical flow regime: ——, present theory, $\beta_S = 104°$, $C_D = 0{\cdot}70$; —·—, present theory, $\beta_S = 100°$, $C_D = 0{\cdot}71$; – – –, theory of Parkinson & Jandali (1970), $\beta_S = 104°$, $C_D = 0{\cdot}79$; ○, experiment of Roshko (1961), Reynolds number $= 8{\cdot}4 \times 10^6$, $C_D = 0{\cdot}70$. (*b*) Critical flow regime: ——, present theory, $\beta_S = 117{\cdot}5°$, $C_D = 0{\cdot}26$; —·—, present theory, $\beta_S = 110°$, $C_D = 0{\cdot}24$; – – –, theory of Parkinson & Jandali (1970), $\beta_S = 117{\cdot}5°$, $C_D = 0{\cdot}34$; ○, experiment of Bearman (1968), Reynolds number $= 2{\cdot}13 \times 10^5$, $C_D = 0{\cdot}31$. θ_f is angle measured from forward stagnation point.

4.3. 90° *wedge*

Through the use of the Schwartz–Christoffel transformation, the mapping function can be written in the form (Parkinson & Jandali 1970)

$$dz/d\zeta = f'(\zeta) = K\zeta(\zeta+1)^{-\frac{1}{4}}(\zeta-1)^{-\frac{3}{4}},$$

where $\zeta = \frac{1}{2}(Z + Z^{-1})$ and K is a scale factor to be determined. Integration of this equation yields

$$z = K\left(\frac{2t^3}{t^4-1} + \tfrac{1}{2}\log\frac{1+t}{1-t} + \frac{i}{2}\log\frac{1+it}{1-it}\right), \tag{37}$$

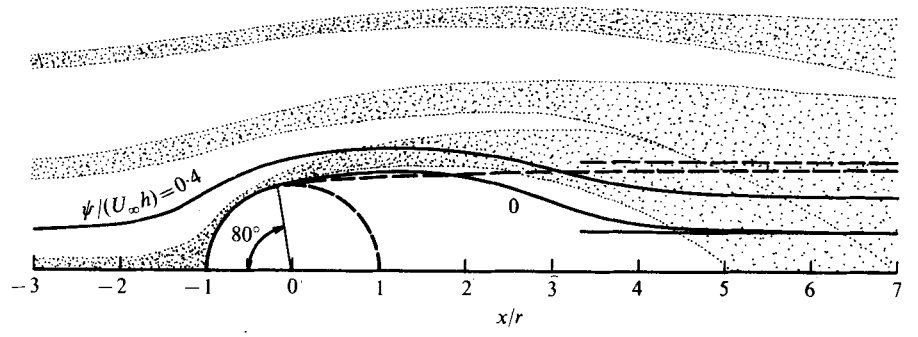

FIGURE 6. Flow pattern around a circular cylinder (subcritical flow regime). ——, present theory, $\beta_S = 80°$; – – –, theory of Parkinson & Jandali (1970), $\beta_S = 80°$. Horizontal lines parallel to x axis show asymptotic height of separation streamlines. r is radius of circular cylinder. Dotted areas show regions contaminated by smoke particles during flow visualization.

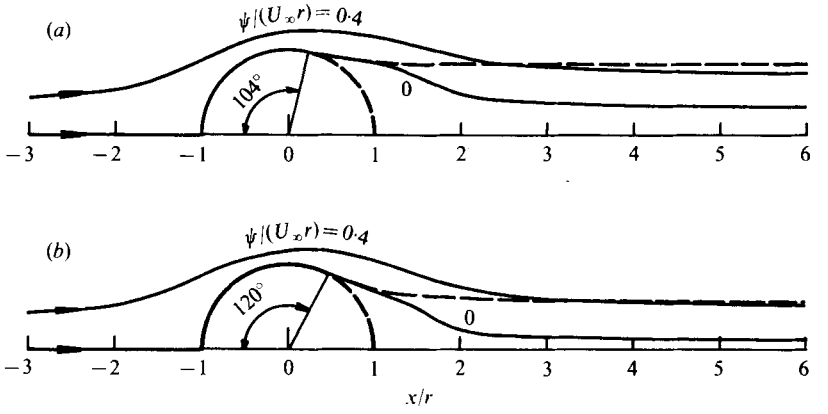

FIGURE 7. Flow pattern around a circular cylinder. (*a*) Critical flow regime: ——, present theory, $\beta_S = 104°$; – – –, theory of Parkinson & Jandali (1970), $\beta_S = 104°$. (*b*) Transcritical flow regime: ——, present theory, $\beta_S = 120°$; – – –, theory of Parkinson & Jandali (1970), $\beta_S = 120°$. r is radius of circular cylinder.

in which $$t = \{(\zeta+1)/(\zeta-1)\}^{\frac{1}{2}} = \{(Z+1)/(Z-1)\}^{\frac{1}{2}}.$$

The transformation (37) maps the upper half of the ζ plane onto the upper half of the z plane, in which the wedge is represented by a slit inclined at 45° to the x axis. The radius of the circle in the Z plane has been taken as unity. The separation points in the Z plane are located at $Z = \pm i$ and thus $\alpha = \frac{1}{2}\pi$. If the height of the wedge is denoted by $2h$, the scale factor K is determined as

$$K = 2h/\{\log\cot\tfrac{1}{8}\pi + \sqrt{2} - \tfrac{1}{2}\pi\}. \tag{38}$$

Since (37) becomes $$z \sim \tfrac{1}{2}KZ + \ldots \quad \text{as} \quad Z \to \infty,$$

one obtains from (3) $$k_1 = 2/K. \tag{39}$$

Furthermore, (38) yields $|f''(Z_{S_1})| = K$. Through the use of these quantities, the parameters Q_1, Q_2 and β can be determined from (10), (16) and (20).

Figure 8 compares the theoretical surface pressure distributions computed by the present method and that of Parkinson & Jandali (1970) with an experimental dis-

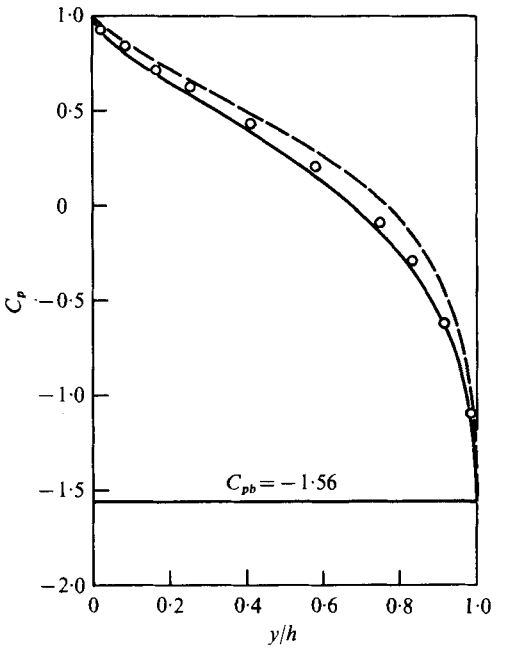

FIGURE 8. Pressure distribution on a 90° wedge. ——, present theory, $C_D = 1{\cdot}74$; – – –, theory of Parkinson & Jandali (1970), $C_D = 1{\cdot}85$; ○, experimental data taken from Parkinson & Jandali (1970), $C_D = 1{\cdot}78$. y is distance measured from forward stagnation point along wedge surface and $2h$ is height of wedge.

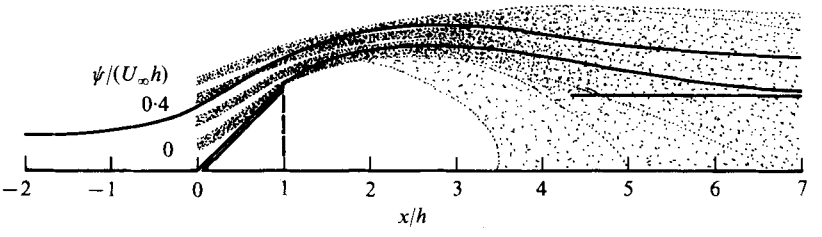

FIGURE 9. Flow pattern around a 90° wedge. ——, present theory. Horizontal line parallel to x axis is asymptotic height of separation streamline. Dotted areas show regions contaminated by hydrogen bubbles during flow visualization.

tribution which is given in their paper. Although both theoretical curves agree quite closely with the experimental values, the present theory may be seen to yield somewhat better agreement. The predicted separation streamline is shown in figure 9 together with an experimental flow pattern taken from a flow-visualization photograph for a Reynolds number of 2100, the exposure time being 10 s. The Reynolds number in this case is defined in terms of the base height of the cylinder ($2h = 50$ mm) and the approach velocity ($U_\infty = 5{\cdot}0$ cm/s). The experiment was performed in a recirculating water channel, the flow around the wedge being visualized with hydrogen bubbles. It seems that the theoretical separation streamline is a fairly good approximation to the displacement surface of the wake, although a more detailed comparison between the theory and experiment should be made on the basis of reliable velocity measurements in the near wake of the wedge.

5. Concluding remarks

An inviscid bluff-body wake model which appropriately takes into account the displacement effect of the far wake has been developed. The present theory, which incorporates some of the ideas underlying the wake source model of Parkinson & Jandali (1970), yields a reasonably good description of the irrotational flow field outside the wake. The separation streamlines obtained from the present theory could be interpreted as the displacement surface of the wake throughout the region of flow from the near wake to the far wake. It should be pointed out that, as far as the authors are aware, almost all of the previous inviscid wake models failed to give definite physical meaning to the separation streamlines far downstream of the body to the same extent as the present theory, although the separation streamlines predicted by these theories agreed fairly well with the time-averaged shear layers within a small distance downstream of the body.

The solutions which were worked out for a normal flat plate, a circular cylinder and a 90° wedge showed that the surface pressure distributions obtained by the present theory gave fairly good agreement with experimental measurements. Furthermore, the theoretical separation streamlines are not inconsistent with displacement surfaces obtained from flow-visualization results.

Bearman & Fackrell (1975) presented a generalization of Parkinson & Jandali's wake source model which extends its applicability to arbitrary two-dimensional and axisymmetric bluff bodies by representing the wetted surface by a distribution of discrete point vortices. By applying the method of Bearman & Fackrell, it may be possible to extend the present theory to body shapes for which suitable transformation functions are not known or difficult to obtain. However this will be left for another study.

The authors express their sincere thanks to Dr T. Igarashi of the Japan Defense Academy for supplying them with the photograph of flow around a circular cylinder from which figure 6 of the present paper was constructed. Figure 9 was prepared from a photograph taken by M. Furukawa, a graduate student at the authors' laboratory of fluid mechanics, Hokkaido University. A referee is also acknowledged for comments which have led to improvement of the paper.

REFERENCES

ARIE, M. & ROUSE, H. 1956 Experiments on two-dimensional flow over a normal wall. *J. Fluid Mech.* **1**, 129.

BATCHELOR, G. K. 1967 *An Introduction to Fluid Dynamics.* Cambridge University Press.

BEARMAN, P. W. 1968 The flow around a circular cylinder in the critical Reynolds number regime. *Nat. Phys. Lab. Aero. Rep.* no. 1257.

BEARMAN, P. W. & FACKRELL, J. E. 1975 Calculation of two-dimensional and axisymmetric bluff-body potential flow. *J. Fluid Mech.* **72**, 229.

BRADBURY, L. J. S. 1976 Measurements with a pulsed-wire and a hot-wire anemometer in the highly turbulent wake of a normal flat plate. *J. Fluid Mech.* **77**, 473.

FAGE, A. & JOHANSEN, F. C. 1927 On the flow of air behind an inclined flat plate of infinite span. *Proc. Roy. Soc.* A **116**, 170.

IGARASHI, T. 1975 Flow and heat transfer around a circular cylinder with slit. [In Japanese]. *Japan Soc. Mech. Engrs Preprint* no. 750–20, p. 145.

PANKHURST, R. C. & HOLDER, D. W. 1952 *Wind-Tunnel Technique. An Account of Experimental Methods in Low- and High-Speed Wind Tunnels.* Pitman.

PARKINSON, G. V. & JANDALI, T. 1970 A wake source model for bluff body potential flow. *J. Fluid Mech.* **40**, 577.

ROSHKO, A. 1954 A new hodograph for free streamline theory. *N.A.C.A. Tech. Note* no. 3168.

ROSHKO, A. 1961 Experiments on the flow past a circular cylinder at very high Reynolds number. *J. Fluid Mech.* **10**, 345.

WOODS, L. C. 1955 Two-dimensional flow of a compressible fluid past given curved obstacles with infinite wakes. *Proc. Roy. Soc.* A **227**, 367.

WOODS, L. C. 1961 *The Theory of Subsonic Plane Flow.* Cambridge University Press.

WU, T. Y. 1962 A wake model for free-streamline flow theory. Part 1. Fully and partially developed wake flows past an oblique flat plate. *J. Fluid Mech.* **13**, 161.

WU, T. Y. 1972 Cavity and wake flows. *Ann. Rev. Fluid Mech.* **4**, 243.